

Interference between Raman gain and four-wave mixing in cold atoms

Franck Michaud,¹ Giovanni-Luca Gattobigio,^{1,2} Jose W. R. Tabosa,³ and Robin Kaiser^{1,*}

¹*Institut Non Linéaire de Nice, UMR 6618 CNRS, 1361 route des Lucioles, F-06560 Valbonne, France*

²*Dipartimento di Fisica dell'Università di Ferrara and Istituto Nazionale di Fisica Nucleare Sezione di Ferrara, 44100 Ferrara, Italy*

³*Departamento de Física, Universidade Federal de Pernambuco, Avenida Professor Luiz Freire, s/n Cidade Universitária, 50670-901 Recife PE, Brazil*

*Corresponding author: Robin.Kaiser@inln.cnrs.fr

Received December 20, 2006; accepted February 27, 2007;
posted March 20, 2007 (Doc. ID 78215); published July 26, 2007

Using a pump–probe scheme with a large cloud of cold rubidium atoms, we observe very large double-pass gain (1800%) due to interference between Raman gain and four-wave mixing. A simple model explains the main features observed. © 2007 Optical Society of America
OCIS codes: 030.6600, 140.3320.

1. INTRODUCTION

The search for strong localization [1] of waves in random media has intensified with the discovery that electromagnetic waves can be used to study the disorder-driven phase transition [2] without the effect of interactions that are important for electrons and Bose–Einstein condensates, for example [3–6]. Many interesting experiments have been performed to approach this phase transition, ranging from the coherent backscattering of light [7–9], to the study of fluctuations [10] with a variety of samples, including laser cooled atoms [11]. Recent progress has been made using time-resolved techniques [12] shown earlier in [13], allowing to discriminate strong localization from absorption, as discussed for previous work [14–16].

It also became clear that using an active sample (with gain) makes it possible to study new, interesting interference effects in multiple scattering, even when the threshold for strong localization in the passive system cannot be achieved. A system combining gain and multiple scattering has been named the “photonic bomb” or “random laser.” Such a system had been proposed many years ago [17] but the field of random lasers has emerged after the more recent experimental work [18]. One of the current hot topics is the so-called coherent random laser, where interference effects in multiple scattering in the gain medium leads to new features, such as distinctive spikes in the emission spectrum [19]. Discriminating between such interference effects and anomalous intensity effects might help us understand the interplay of localization effects and gain.

Since most samples used in this context are either dyes with colloidal suspension or semiconductor powders, some aspects, such as the occurrence of long-range correlation between the optical coherence of the radiating dipoles, leading to superfluorescence, could not have been investigated as yet. We propose to use a sample of laser-cooled

atoms to study random lasers with large optical coherence lifetime. In the past, such samples have been used in the absence of gain to investigate coherent backscattering of light by resonant scatters [11,20,21]. Narrow resonances in such samples yield new features such as the dispersion and time dependence of multiple scattering [22]. It is also known that such samples of laser-cooled atoms can be used to produce a sample with gain [23]. Various gain mechanisms can be used with cold atoms, such as Mollow gain [24], Raman gain [25–28], or recoil-induced resonance [29,30]. In the past, only moderate single-pass gain has been obtained with cold atoms, mainly limited because of the reduced optical thickness of the samples that could be realized. Even with such moderate gain, fascinating experiments have been realized, allowing the study of nonclassical effects of atom lasers [31,32] or collective atomic recoil lasers [33]. Using clouds with a larger number of atoms and increased optical thickness, it is, however, possible to obtain large gain [34] even in the absence of cavities.

In this paper, we present a new mechanism to the best of our knowledge, for producing significant gain without relying on a high-finesse cavity. As in most pump–probe experiments with cold atoms, the pump beam needs to be in a counterpropagating configuration in order to balance the radiation pressure. One thus naturally has a system in which four-wave mixing (FWM) is expected [35]. We will show in this paper how the Raman gain in the forward direction can interfere with the conjugate beam produced by FWM to yield a double-pass gain of 1800%. This paper is organized as follows. First we describe our experimental setup in Section 2. The results of nondegenerate four-wave mixing (NDFWM) are presented in Section 3; those of single-pass gain in Section 4. The most important result of this paper, i.e., the important double-pass gain, is presented in Section 5.

2. EXPERIMENTAL SETUP

The experiment was performed in a sample of cold rubidium atoms in a magneto-optical trap (MOT). Our MOT scheme has been described elsewhere [11] and allows time-controlled switching of the trapping and repumping beams as well as of the magnetic quadrupole field. One particular aspect of our trap is the large number of atoms ($N_{\text{at}} \approx 10^{10}$) that can be trapped, due to large beam waists and the corresponding large powers for the trapping and cooling lasers. In a previous experiment, we have investigated degenerate four-wave mixing (DFWM) and described a bunching-induced red–blue asymmetry in the DFWM spectra [35]. In contrast to those experiments in which all DFWM beams were provided by the same laser (frequencies $\omega_F = \omega_B = \omega_P$), we have added an independent probe beam P , allowing us to study the dependence of the relative detuning $\delta = \omega_P - \omega_F$ of our signals. The pump beams are independent (not retroreflected) carefully aligned counterpropagating pumping beams (forward F and backward B). The angle between the probe (P) and forward beam (F) has been kept constant at ~ 0.2 rad. The waist of the laser beams ($w_{F,B} = 3$ mm, $w_P = 1.7$ mm/FWHM $_P \approx 2$ mm) is smaller than the size of our cloud ($L_{\text{rms}} \approx 2$ mm/FWHM ≈ 4.7 mm). The polarization of the DFWM beams can be adjusted by appropriate wave plates and polarizing cubes placed along the beam paths. In the work reported in this paper, we have used the $F \parallel B \perp P$ polarization configuration, in which the two pump beams F and B have linear and parallel polarizations and the probe beam P has a linear polarization orthogonal to the pump polarization. We define saturation

parameters s_F , s_B , and s_P for the forward and backward pump and the probe beam by the beam center intensity divided by the saturation intensity $I_{\text{sat}} = 1.6$ mW/cm 2 of the $F=3 \rightarrow F'=4$ transition of ^{85}Rb . The MOT trapping beam and magnetic field gradient are switched off for ~ 1 ms every 30 ms and the pump and probe field act on atoms unperturbed by the MOT preparation (see Fig. 1).

Spectra are obtained by sweeping the probe frequency with respect to the pump frequency, which has been kept at fixed detuning, $\Delta = \omega_{F,B} - \omega_{\text{at}}$, with respect to the atomic resonance of the $F=3 \rightarrow F'=4$ of the D_2 line of ^{85}Rb . We have checked that the duration of the frequency ramp (of the order of 20–100 μs) is long enough not to limit the width of the recorded resonances and short enough not to lose atoms during the exposure to the large intensity pump fields. The independent probe beam P is generated from the same master laser as the pump fields F and B using different acousto-optical modulators to control the frequency difference. The stability of the probe frequency versus pump frequency has been checked by radio-frequency analysis and by the laser beatnote to be of the order of 20 kHz during one probe pulse duration and less than 100 kHz over a second, corresponding to the typical averaging time used for the signals reported in this paper. Fast and sensitive detection is obtained with use of a channel photomultiplier.

3. NDFWM

To realize a gain medium, one obviously needs to pump energy into the sample. This is achieved with optical pumping using strong quasi-resonant pump fields F and B (see Fig. 1). Since cold atoms are sensitive to radiation pressure forces, it is convenient to use counterpropagating pump beams to balance the radiation pressure forces. This makes this pump–probe scheme similar to a backward FWM configuration, which we have used previously [36]. Since we are interested in the gain spectrum of our system, we have recorded the NDFWM signal, i.e., we have recorded the backward FWM as a function of the probe–pump detuning δ for a fixed-pump frequency Δ . In Fig. 2, we show the resulting NDFWM signal obtained with a large cloud of cold atoms. The data shown here focus on a narrow frequency range around the pump–probe resonance, corresponding to the central feature of [36]. The width of the NDFWM is of the order of several times 100 kHz, consistent with the Doppler width of our atomic sample. The main point to notice here is the large value of NDFWM ($\approx 80\%$) of the incident probe beam that can be obtained. This will be important for the double-pass gain described later in the paper. A moderate increase in the optical thickness of our cloud might allow us to obtain a FWM yield larger than unity in the future. A regime similar to the self-oscillation in FWM in sodium [37] or the mirrorless oscillation observed with nonlinear materials [38,39] could then be obtained with this sample. Although such mirrorless oscillation is not discussed in the context of a random laser (another mirrorless oscillator), both situations are based on nonlinear matter–light interactions and might have to be considered when trying to understand the combination of multiple scattering and gain.

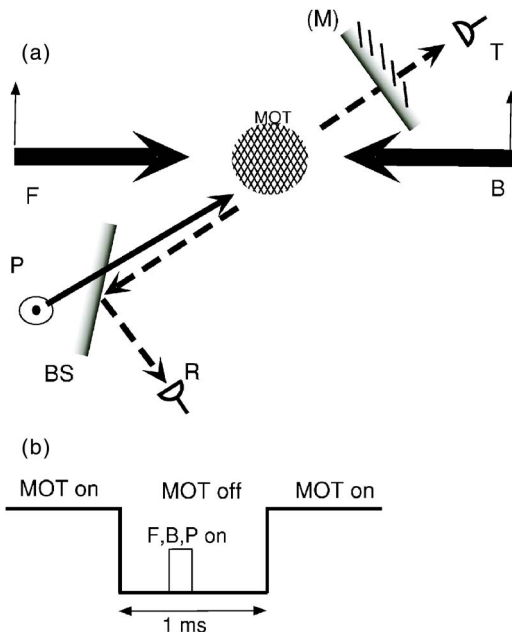


Fig. 1. (a) Schematic of the experiment: two strong counterpropagating pump beams (F and B with parallel linear polarization) and one weak probe beam (P with linear polarization orthogonal to that of F and B) are applied; an additional mirror (M) has been used for double-pass gain (see text) and either transmission (T) or reflection (R) through a beam splitter (BS) has been recorded; (b) timing of the experiment: the MOT beams and magnetic fields are switched off during the short pump–probe pulse.

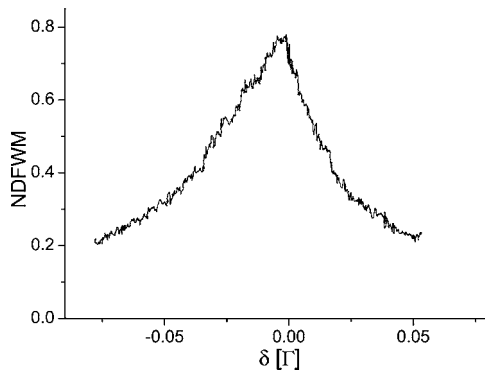


Fig. 2. NDFWM spectrum obtained in the $F\parallel B\perp P$ configuration. The pump frequency ($\Delta=-4.8\Gamma$) and intensity ($s_{F,B}=23$, $s_P=0.01$) are kept fixed as the detuning $\delta=\omega_P$ of the probe beam P is scanned across the NDFWM resonance. Note that the scale of the detuning scan shown here is covering a smaller range than in the subsequent figures.

4. SINGLE-PASS GAIN

In a first series of experiments, we measured the gain that can be obtained in our sample and identified the dominant gain mechanism. Indeed, several gain mechanisms can exist in such systems: (i) Mollow gain one would expect from a strongly driven two-level system, (ii) mechanical assisted gain at work in recoil-induced resonances and/or vibrational Raman resonances, or (iii) stimulated Raman transitions between different Zeeman sublevels. As we will show below, the last mechanism is the dominant gain in our experiment.

The very rich physics of pump-probe spectroscopy with cold atoms was a dynamic field of research in the beginning of the 1990s and a lot of results are summarized in a review paper [23]. The transmission through a cloud of atoms increases exponentially with the number of atoms, as illustrated by the important recoil-induced resonances-based gain obtained in an elliptically shaped optical thick cloud of atoms [36]. Our results, obtained with a different geometry for the cloud and the laser beams, are dominated by Raman transitions between different Zeeman sublevels.

Despite the above-mentioned sensitivity of cold atoms to radiation pressure, the radiation pressure forces are not strong enough to accelerate the atoms out of resonance during the interaction with the pump and probe beams for the smaller interaction times we have used (below $40\ \mu\text{s}$). Spatial displacement of the atoms is less important since it would take an even longer time to displace the atoms by more than the initial cloud size. We have thus been able to record the transmission of the probe beam in the presence of a single pump beam (F or B). A typical gain spectrum is shown in Fig. 3.

The transmission of a low-intensity probe beam is recorded with either pump beam F or pump beam B on. One can clearly see that gain is obtained only with the co-propagating F pump [Fig. 3(a)], whereas the counter-propagating B pump does not produce net gain [Fig. 3(b)]. The resonance condition for the Raman gain is fulfilled when the probe-pump detuning δ is equal to the energy difference of the Zeeman sublevels coupled via this two-photon process. In the absence of a magnetic field, the en-

ergy of the Zeeman sublevels is determined by the light shift induced by the strong pump beams. The coupling strength of the various Zeeman sublevels depends on the Clebsch-Gordan coefficients and for the $F=3-F'=4$ transition in this work, the pump-induced light lifts the degeneracy of the $F=3$ state. To verify that the resonance condition is given by the energy difference of the Zeeman levels, we have also added a pulsed-bias field (only when the pump and probe are switched on) and have indeed observed that the resonance condition in that case depends on the applied-bias field. The shape and the number of resonances can be drastically altered in the presence of a bias field, and in the future we might exploit this controlled dependence of the resonance condition combined with optical Zeeman pumping for optimizing the properties of our system for the realization of a random laser with cold atoms.

One signature of the Raman gain mechanism in contrast, e.g., to the recoil-induced resonances is that gain for negative pump detuning ($\Delta<0$) is obtained for a probe frequency below the pump frequency ($\delta<0$), whereas for $\Delta>0$, gain is obtained for $\delta>0$. This is explained by the fact that the Zeeman sublevel most shifted by light is also the most populated (see Fig. 4) on an $F-F'=F+1$ transition. The difference between the gain obtained with the

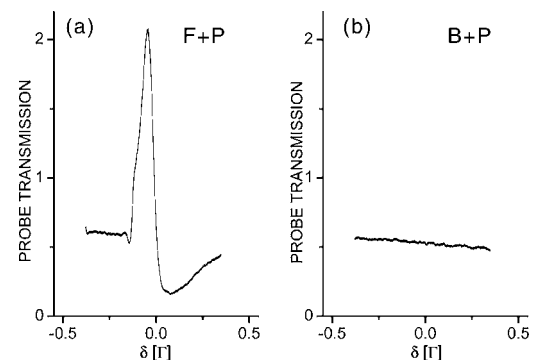


Fig. 3. Gain spectrum for $F\parallel B\perp P$ polarization. (a) for the quasi-co-propagating pump (F) and probe (P) beams ($s_F=30$ and $\Delta=-3\Gamma$). A distinctive gain of $\sim 100\%$ is seen at the Raman condition, for $\delta=\omega_{\text{Raman}}$. (b) For the quasi-counter-propagating pump (B) and probe (P) beams ($s_B=30$ and $\Delta=-3\Gamma$) no gain is observed.

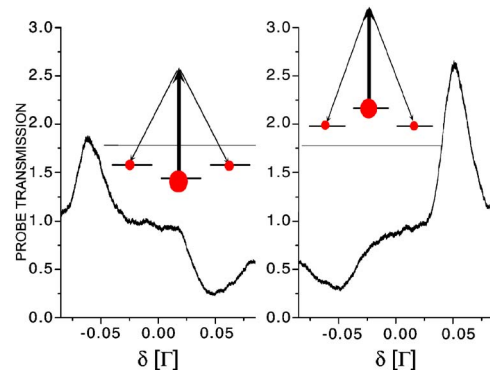


Fig. 4. (Color online) Raman gain mechanism. (a) Gain spectrum for negative pump detuning and corresponding gain spectrum ($\Delta=-5.2\Gamma$, $s_F=30$, $s_P=0.07$). (b) Gain spectrum for positive pump detuning and corresponding gain spectrum ($\Delta=+5.2\Gamma$, $s_F=30$, $s_P=0.07$). Insets indicate the different light shifts and populations corresponding to the gain part of each curve.

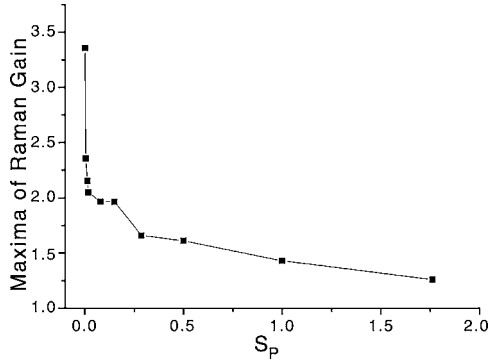


Fig. 5. Gain saturation. Maximum of the gain spectra for different probe intensities at fixed-pump parameters ($s_F=6.8$ and $\Delta=-3\Gamma$).

copropagating and the counterpropagating pump beam can be explained by the residual Doppler broadening for the two-photon process involving quasi-co-propagating (F and P) or quasi-counter-propagating fields (B and P) [40,41].

The combination of these signatures shows that the dominant gain mechanism in the experiments reported in this paper is the Raman gain between different Zeeman sublevels. Other gain mechanisms, in particular recoil-induced resonances (or its equivalent for trapped atoms, i.e., Raman transitions between different vibrational levels), can also contribute to the signal. We have indeed observed a narrower central feature for lower saturation and atom numbers. However, we attribute the dominant gain feature in our experiment to Raman gain between different Zeeman sublevels.

We have also performed a more systematic study of single-pass Raman gain. When the probe intensity is increased, one obtains lower gain. This gain saturation is illustrated in Fig. 5 where one can see that probe intensity below $0.01I_{sat}$ ($s_P < 0.01$) is required for optimal gain. We do not expect this gain saturation to be a limiting factor for a laser using this gain mechanism, since such a laser would be triggered by low-intensity spontaneous emission. However, the intensity that can be expected from such a laser in steady state would be determined by non-linear effects such as this gain saturation mechanism.

Another feature of gain using cold atoms is the exponential increase with the increasing optical thickness of the cloud, as, e.g., mentioned in [34]. However, the gain cannot be described only by the optical thickness at the frequency of the pump and probe beams. Indeed, even though gain does increase with the number of atoms (see Fig. 6), it is reduced around resonance as shown in Fig. 7. Several effects contribute to the reduced gain around resonance.

First, even for an optically thin cloud of atoms, the gain is predicted to have a more complex dependence on the detuning. Indeed, gain is turning into absorption as the pump detuning Δ is scanned across the atomic resonance. Following previous work [42], we expect

$$g \propto e^{N_{at}(\pi_a - \pi_b)f(\delta)}, \quad (1)$$

where π_a and π_b are the populations of the two Zeeman levels coupled via the two-photon pump-at probe transi-

tion and $f(\delta)$ is a function that depends on the pump intensities (s_F, s_B) as well as on the pump detuning Δ and on the details of the atomic transition. A simplified understanding of the function can be obtained by considering the function

$$f(\delta) = \frac{A_1}{(\delta - \omega_{\text{Raman}})^2 + \gamma^2/4} - \frac{A_2}{(\delta + \omega_{\text{Raman}})^2 + \gamma^2/4}, \quad (2)$$

where γ describes the width of the Raman gain and A_1 and A_2 describe the weights of the gain and absorption processes, respectively. All these parameters depend on the intensities of the pump and probe beams as well as on the pump detuning, Δ . The coefficients A_1 and A_2 differ since the strength of the two-photon process involving either “pump absorption and probe emission” or “probe absorption and pump emission” is not the same due to a difference in the Clebsch–Gordan coefficients. As a result of the $F=3-F'=4$ transition used in our Rb experiment, a more precise model needs to account for multiple two-photon transitions with each at a different resonance position and width. The net result is an overall inhomogeneous broadening of the resonance [23]. The precise origin of the width γ of the Raman resonances has, however, been much debated [23] and can involve the inhomogeneous broadening due to different energy splitting of all levels involved, the finite temperature of the atoms, optical pumping from one sublevel into another, but a reduced width can also be present in the case of strong atomic localization in the bottom of the potential well (Lamb–Dicke narrowing).

The influence of the number of atoms beyond that described by Eq. (2) also needs to be considered. Indeed, we have observed significant broadening of gain spectra as the number of atoms is increased. With increased atom number, the width γ of the resonances are no longer small compared with their separation $2\omega_{\text{Raman}}$; reducing the maximum gain that can be obtained. Even though using a large number of atoms is obviously desirable for large gain, it makes a quantitative comparison with an *ab initio* model more difficult.

The net result for the maximum gain is shown in Fig. 7, where a significant reduction of the gain is observed close to the center of the atomic resonance. Using this gain to build a standard cavity laser, one should therefore choose off-resonant pumping. However, this center line reduction

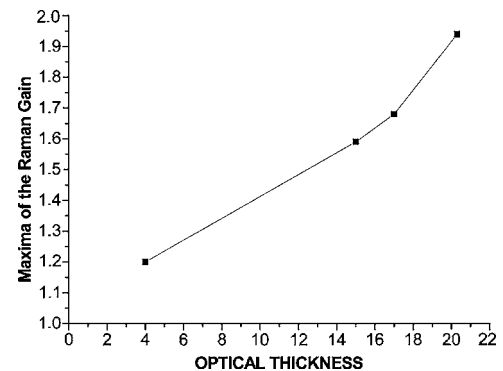


Fig. 6. Maximum of gain spectra as a function of the (resonant) optical thickness of the cloud, varied by changing the atom number ($s_F=30$, $\Delta=-3\Gamma$, and $s_P=0.07$).

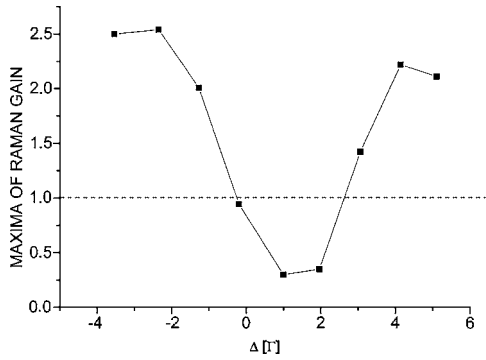


Fig. 7. Maximum of gain spectra as a function of pump detuning Δ at maximum atom number ($N_{\text{at}}=10^{10}$) for $s_F=30$ and $s_P=0.07$.

of the gain is also due to multiple scattering in the optically thick cloud of atoms. The combination of multiple scattering and gain is the route to follow to realize a random laser with cold atoms. One important aspect to study is the separate control of gain and multiple scattering, since the scattering mean free path in cold atoms will be affected by the pump lasers. In this respect, the Raman gain mechanism seems to be more promising than the other possible gain mechanisms mentioned above (Mollow gain or mechanical-assisted gain). Indeed, a single frequency of the propagating field will be amplified by some of the Zeeman sublevels (corresponding to negative absorption or a negative mean free path) whereas other Zeeman sublevels will not contribute to the gain and will thus contribute to the scattering (with a positive mean free path). The other gain mechanisms can be explained with a two-level atomic model, and thus the mean free path for one frequency of the propagating field will be either positive or negative, making the combination of gain and multiple scattering a more difficult task, required to realize a random laser. With the Raman gain presented in this paper, it might be possible to control the relative amounts of gain and scattering and also combine both by controlling the populations of the different Zeeman sublevels.

5. DOUBLE-PASS GAIN

Having understood the origin of our gain in a single-pass configuration, we investigated the extent to which this gain can be increased in a multipass configuration. For this purpose, we reflect the probe beam with a mirror (see Fig. 1) and recorded the intensity on the same detector used in the NDFWM experiment. This configuration might also make it possible to achieve random lasing in our system. Indeed, if one can approach the threshold for a random laser, i.e., when amplified emission can occur in each direction, adding a single mirror will increase the total gain in one of these directions. One might thus be able to detect emission in the direction specified by the mirror, even in the absence of a probe beam. We have not investigated this possibility as yet, since our goal was to understand the amplification of a probe beam.

To our surprise, the double-pass gain with a probe beam became very sensitive to small adjustments in the mirror alignment as well as to the alignments of the

pump beams F and B . Also, very distinctive chirped oscillations appear in the double-pass spectrum (see Fig. 8). A third remarkable feature is the giant double-pass gain obtained, up to 1800%. Let us now turn to the explication of these features, which we will use in future work for realizing a cavity-type laser as well as for a random laser with cold atoms.

The oscillations in the double-pass spectrum of Fig. 8 can easily be understood by noting that the frequency of the conjugate beam is not identical to that of the incident probe beam. Indeed the FWM condition yields a beam of frequency:

$$\omega_C = 2\omega_{F,B} - \omega_P. \quad (3)$$

At resonance, $\omega_P = \omega_{F,B}$, the conjugate and probe beams have the same frequency, but as the probe frequency is tuned further from resonance, the frequency difference between the conjugate and probe beam increases. On the other hand, the transmitted beam (with Raman gain) is at the same frequency as the incident probe beam, since the gain is a stimulated emission process into the mode of the probe beam. When detecting in the backward direction in the presence of a mirror, we will get the result of NDFWM as well as double-pass Raman gain. When the mirror is carefully aligned, these two fields interfere, and the resulting beat note is the origin of the oscillations in Fig. 8. Also, the relative phase of the interfering beams now depends on the distance between the atomic cloud and the mirror. This cavitylike sensitivity explains the large shot-to-shot fluctuations observed on the signal at approximately $\delta=0$.

A more detailed analysis indicates that multipass effects must be taken into account, since the beam that is reflected off the mirror can produce a conjugate beam by itself and return to the mirror. In some sense, the quite large reflection coefficient we have described in a previous section produces a low-finesse cavity made by the mirror and the atomic sample. This cavity-type behavior makes our signal very sensitive to small fluctuations of, e.g., the mirror positions. We now need to include more than two fields to compute the total signal in the backward direction. Our model thus includes multiple reflections with frequency changes each time a beam is transformed into a conjugate beam. We denote by r_c the amplitude of the reflection coefficient off the atom cloud (i.e., the FWM con-

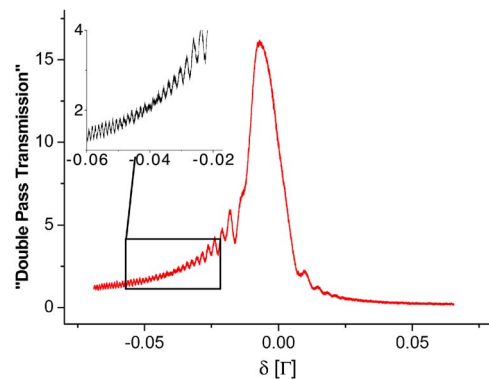


Fig. 8. (Color online) Double-pass gain spectrum as a function of pump detuning δ ($\Delta=-4.5\Gamma$, $s_{F,B}=23$, $s_P=0.01$ at maximum atom number $N_{\text{at}}=10^{10}$).

version efficiency), and t_F , t_B denote the amplitudes of the transmission coefficients through the atom cloud along the incoming path and reflected paths of the probe beam, respectively. This notation suggests that the Raman gain is dominated by the copropagating pump beam, as described in Section 4. We also assume, $t_F = t_B$, thus neglecting cross saturation and/or absorption effects. The incoming probe beam is denoted, $E_{\text{inc}} = E_0 e^{i\omega_p t}$.

For a single interaction with the atomic cloud, the transmitted signal becomes $t_F E_0 e^{i\omega_p t}$, and the reflected signal $r_c E_0^* e^{i(\omega_p - 2\delta)t}$ is the conjugate signal of the incoming beam. We have computed the total reflected field in two different ways. First, we only consider the interference between the conjugate beam and the beam transmitted twice through the atomic cloud. The corresponding normalized signal is then given by

$$I_1 = |r_c e^{i(\omega_p - 2\delta)t} + t_F t_B e^{i\omega_p t} e^{i\phi}|^2, \quad (4)$$

where the phase factor $\phi = 2kL$ describes that phase difference of the beam between the atomic cloud and the mirror at a distance L .

In the experiment, we sweep the probe frequency, and δ becomes a function of time: $\delta = \alpha t$, with α of the order of $10^{-4} \text{ } \Gamma/\mu\text{s}$. The fast oscillations of Fig. 8 arise from the interference term $\cos(2\alpha\delta^2)$. We have verified in the experiment that the peak-to-peak distance of these oscillations follows a $1/\delta$ law, as expected. Also, due to Raman absorption for $\delta > 0$ ($\Delta < 0$), oscillations are strongly reduced since the amplitude of one interfering beam is very small. One interesting feature is the minimum in the contrast of the oscillations at approximately $\delta \approx -0.04\Gamma$ close to the maximum of the Raman gain (see the inset in Fig. 8). This feature can be explained by the π phase of the Raman resonance and illustrates the rich physics involved in this double-pass gain experiment.

A second, more complete analysis also includes multiple reflections between the atomic cloud and the back mirror. Since the frequency of the reflected beam flips around the pump frequency at each reflection off the atomic cloud, the total field can be written as

$$I_2 = \left| r_c e^{i(\omega_p - 2\delta)t} + t_F t_B \sum_n r_c^{2n} e^{2ni\phi} e^{i\omega_p t} + t_F t_B \sum_n r_c^{2n+1} e^{(2n+1)i\phi} e^{i(\omega_p - 2\delta)t} \right|^2. \quad (5)$$

In Fig. 9, we show the result of our simulations following Eqs. (4) and (5). When comparing the maximum gain obtained in our experiment with our model, we see that several reflections between the atomic cloud and the mirror need to be included to produce a total gain of 1800%, i.e., a transmission of the probe beam of 18. Indeed a single interference of a beam with a relative intensity of 0.8 and one with an intensity of 2 cannot produce the observed gain. With the FWM efficiency of 0.8, one can, however, see the atomic cloud and the back mirror as a low-finesse cavity of approximately $F=20$ (including roundtrip losses on the uncoated interfaces of the vapor cell). The large double-pass gain observed in our experiment can be explained by including these multiple reflections between the atomic cloud and the mirror. Also, the maximum of the total signal is closer to the maximum of

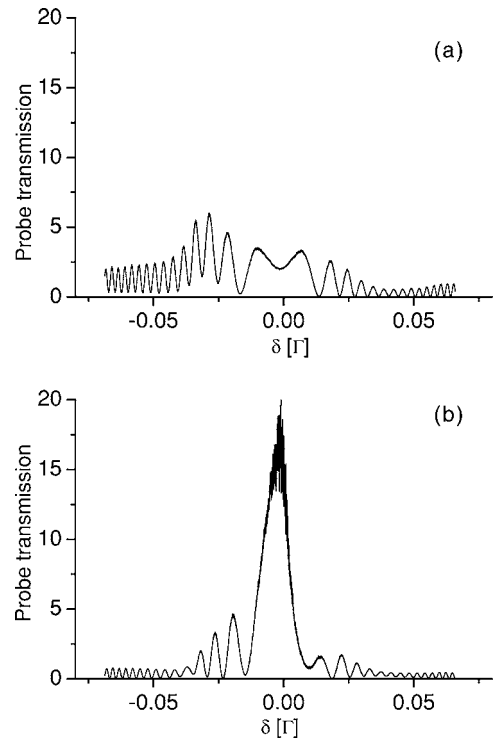


Fig. 9. Simulated double-pass gain spectrum using the experimental FWM result and Raman gain curve as input. (a) Only one interference term between the FWM and the Raman gain is included [see Eq. (4)]. (b) Multiple reflections between the atomic cloud and the back mirror are included [see Eq. (5)]. The signal depends crucially on the distance between the atomic cloud and the mirror ($L \approx 0.2 \text{ m}$).

the NDFWM signal, consistent with the important role played by this effect. We notice, however, that the contrast of the oscillations for $\delta < 0$ is clearly larger than observed in the experiment, and a maximum is not reached around the Raman resonance. We speculate that these reductions can be due to the convolution of the signal with the velocity distribution $f(v)$ of the atoms and by fluctuations of the cavity length during the integration of the signal (typically of the order of seconds). Indeed, Doppler broadening is of the order of 100 kHz, which can reduce the contrast of the faster oscillations of the interferences described by Eq. (5). We also notice important sweep-to-sweep fluctuations in the signal and the oscillations as well as the significant gain at the FWM resonance is strongly attenuated when long integration times have been used. Fluctuations of the mirror position can be reduced by better mechanical stability, and the Doppler broadening could be reduced by almost 1 order of magnitude by applying a molasses phase before the pump-probe beams.

6. CONCLUSION

In this paper, we have presented pump-probe experiments performed on a large cloud of cold atoms and identified the dominant gain mechanism as due to Raman transitions between different Zeeman sublevels. This gain mechanism might be of future interest to realize a random laser with cold atoms. We have observed an unexpected large gain in a double-pass configuration, due to

multiple four-wave mixing reflections between the atomic cloud and the mirror interfering with the Raman gain. This large gain should allow us to build a Fabry–Perot-type laser with cold atoms as the gain medium. This laser might present interesting features, since gain is based on a combination of mechanisms. The work presented in this paper thus opens the way for a variety of lasers that can be realized. If gain as presented in this work can be combined with larger atomic densities, one could also investigate the effect of coherent multiple scattering in the presence of gain when approaching the threshold of strong localization. Indeed, it would be interesting to study to what extent gain allows the observation of precursors of strong localization farther away from the localization threshold of passive systems. At present, however, two challenging tasks, i.e., combining gain and multiple scattering in a dilute system on one hand and reaching the threshold of localization in passive systems on the other hand, are investigated along separate routes.

ACKNOWLEDGMENTS

We thank G. Labeyrie for valuable help on the experimental setup. We acknowledge the financial support of CNRS and of the PACA Region. F. Michaud is funded by Direction Generale de l'Armement. J. W. R. Tabosa acknowledges CNRS, CAPES-COFECUB, and Conselho Nacional de Desenvolvimento Científico e Tecnológico for travel support.

REFERENCES

1. P. W. Anderson, "Absence of diffusion in certain random lattices," *Phys. Rev.* **109**, 1492–1505 (1958).
2. S. John, "Strong localization of photons in certain disordered dielectric superlattices," *Phys. Rev. Lett.* **58**, 2486–2489 (1987).
3. D. Clément, A. Varón, M. Hugbart, J. Retter, P. Bouyer, L. Sanchez-Palencia, D. Gangardt, G. Shlyapnikov, and A. Aspect, "Suppression of transport of an interacting elongated Bose–Einstein condensate in a random potential," *Phys. Rev. Lett.* **95**, 170409 (2005).
4. C. Fort, L. Fallani, V. Guarrera, J. Lye, M. Modugno, D. Wiersma, and M. Inguscio, "Effect of optical disorder and single defects on the expansion of a Bose–Einstein condensate in a one-dimensional waveguide," *Phys. Rev. Lett.* **95**, 170410 (2005).
5. J. E. Lye, L. Fallani, M. Modugno, D. Wiersma, C. Fort, and M. Inguscio, "A Bose–Einstein condensate in a random potential," *Phys. Rev. Lett.* **95**, 070401 (2005).
6. T. Schulte, S. Drenkelforth, J. Kruse, W. Ertmer, J. Arlt, K. Sacha, J. Zakrzewski, and M. Lewenstein, "Routes towards Anderson-like localization of Bose–Einstein condensates in disordered optical lattices," *Phys. Rev. Lett.* **95**, 170411 (2005).
7. P.-E. Wolf and G. Maret, "Weak localization and coherent backscattering of photons in disordered media," *Phys. Rev. Lett.* **55**, 2696–2699 (1985).
8. M. P. van Albada and A. Lagendijk, "Observation of weak localization of light in a random medium," *Phys. Rev. Lett.* **55**, 2692–2695 (1985).
9. Y. Kuga and A. Ishimaru, "Retroreflectance from a dense distribution of spherical particles," *J. Opt. Soc. Am. A* **8**, 831–836 (1984).
10. A. A. Chabanov, M. Stoytchev, and A. Z. Genack, "Statistical approach to photon localization," *Nature* **404**, 850–853 (2000).
11. G. Labeyrie, F. de Tomasi, J.-C. Bernard, C. A. Müller, Ch. Miniatura, and R. Kaiser, "Coherent backscattering of light by cold atoms," *Phys. Rev. Lett.* **83**, 5266–5269 (1999).
12. C. M. Aegerter, M. Störzer, and G. Maret, "Experimental determination of critical exponents in Anderson localization of light," *Europhys. Lett.* **75**, 562–568 (2006).
13. A. A. Chabanov, Z. Q. Zhang, and A. Z. Genack, "Breakdown of diffusion in dynamics of extended waves in mesoscopic media," *Phys. Rev. Lett.* **90**, 203903 (2003).
14. D. S. Wiersma, P. Bartolini, A. Lagendijk, and R. Righini, "Localization of light in a disordered medium," *Nature* **390**, 671–673 (1997).
15. F. Scheffold, R. Lenke, R. Tweer, and G. Maret, "Localization or classical diffusion of light," *Nature* **398**, 206–207 (1999).
16. D. S. Wiersma, J. Gomez Rivas, P. Bartolini, A. Lagendijk, and R. Righini, "Wiersma *et al.* reply," *Nature* **398**, 207 (1999).
17. V. S. Letokhov, "Generation of light by a scattering medium with negative resonance absorption," *Zh. Eksp. Teor. Fiz.* **53**, 1442–1452 (1967) [*Sov. Phys. JETP* **26**, 835–840 (1968)].
18. N. M. Lawandy, R. M. Balachandran, A. S. L. Gomes, and E. Sauvain, "Laser action in strongly scattering media," *Nature* **369**, 436–438 (1994).
19. H. Cao, Y. Xu, S.-H. Chang, and S. T. Ho, "Transition from amplified spontaneous emission to laser action in strongly scattering media," *Phys. Rev. E* **61**, 1985–1989 (2000).
20. Y. Bidet, B. Klappauf, J. C. Bernard, D. Delande, G. Labeyrie, C. Miniatura, D. Wilkowski, and R. Kaiser, "Coherent light transport in a cold strontium cloud," *Phys. Rev. Lett.* **88**, 203902 (2002).
21. D. V. Kupriyanov, I. M. Sokolov, P. Kulatunga, C. I. Sukenik, and M. D. Havey, "Coherent backscattering of light in atomic systems: application to weak localization in an ensemble of cold alkali-metal atoms," *Phys. Rev. A* **67**, 013814 (2003).
22. G. Labeyrie, E. Vaujour, C. A. Müller, D. Delande, C. Miniatura, D. Wilkowski, and R. Kaiser, "Slow diffusion of light in a cold atomic cloud," *Phys. Rev. Lett.* **91**, 223904 (2003).
23. G. Grynberg and C. Robillard, "Cold atoms in dissipative optical lattices," *Phys. Rep.* **355**, 335–451 (2001).
24. F. Y. Wu, S. Ezekiel, M. Ducloy, and B. R. Mollow, "Observation of amplification in a strongly driven two-level atomic system at optical frequencies," *Phys. Rev. Lett.* **38**, 1077–1080 (1977).
25. C. Mennerat-Robilliard, L. Guidoni, K. I. Petsas, P. Verkerk, J.-Y. Courtois, and G. Grynberg, "Bright optical lattices in a longitudinal magnetic field, experimental study of the oscillating and jumping regimes," *Eur. Phys. J. D* **1**, 33–45 (1998).
26. J. W. R. Tabosa, G. Chen, Z. Hu, R. B. Lee, and H. J. Kimble, "Nonlinear spectroscopy of cold atoms in a spontaneous-force optical trap," *Phys. Rev. Lett.* **66**, 3245–3248 (1991).
27. D. Grison, B. Lounis, C. Salomon, J.-Y. Courtois, and G. Grynberg, "Raman spectroscopy of cesium atoms in a laser trap," *Europhys. Lett.* **15**, 149–154 (1991).
28. T. M. Brzozowski, M. Brzozowska, J. Zachorowski, M. Zawada, and W. Gawlik, "Probe spectroscopy in an operating magneto-optical trap: the role of Raman transitions between discrete and continuum atomic states," *Phys. Rev. A* **71**, 013401 (2005).
29. J. Guo, P. R. Berman, B. Dubetsky, and G. Grynberg, "Recoil-induced resonances in nonlinear spectroscopy," *Phys. Rev. A* **46**, 1426–1437 (1992).
30. J.-Y. Courtois, G. Grynberg, B. Lounis, and P. Verkerk, "Recoil-induced resonances in cesium: an atomic analog to the free-electron laser," *Phys. Rev. Lett.* **72**, 3017–3020 (1994).
31. L. Hilico, C. Fabre, and E. Giacobino, "Operation of a 'cold-atom laser' in a magneto-optical trap," *Europhys. Lett.* **18**, 685–688 (1992).
32. A. Lambrecht, J. M. Courty, S. Reynaud, and E. Giacobino, "Cold atoms: a new medium for quantum optics," *Appl. Phys. B* **60**, 129–134 (1995).

33. C. von Cube, S. Slama, D. Kruse, C. Zimmermann, Ph. W. Courteille, G. R. M. Robb, N. Piovella, and R. Bonifacio, *Phys. Rev. Lett.* **93**, 083601 (2004).
34. M. Vengalattore and M. Prentiss, "Recoil-induced resonances in the high-gain regime," *Phys. Rev. A* **72**, 021401(R) (2005).
35. G. L. Gattobigio, F. Michaud, J. Javaloyes, J. W. R. Tabosa, and R. Kaiser, "Bunching induced asymmetry in degenerate four-wave mixing with cold atoms," *Phys. Rev. A* **74**, 043407 (2006).
36. A. Lezama, G. C. Cardoso, and J. W. R. Tabosa, "Polarization dependence of four-wave mixing in a degenerate two-level system," *Phys. Rev. A* **63**, 013805 (2001).
37. M. Pinard, D. Grandclement, and G. Grynberg, "Continuous-wave self-oscillation using pair production of photons in four-wave mixing in sodium," *Europhys. Lett.* **2**, 755–760 (1986).
38. A. Novikov, V. Obukhovski, S. Odoulov, and B. Sturman, "Mirrorless coherent oscillation due to six-beam vectorial mixing in photorefractive crystals," *Opt. Lett.* **13**, 1017–1019 (1988).
39. G. Grynberg, E. le Bihan, P. Verkerk, and M. Ducloy, "Observation of instabilities due to mirrorless four-wave mixing oscillation in sodium," *Opt. Commun.* **67**, 363–366 (1988).
40. J. Guo, "Contribution of energy continuum states to probe the absorption signal of atoms in one-dimensional optical molasses," *Phys. Rev. A* **49**, 3934–3942 (1994).
41. Y.-C. Chen, Y.-W. Chen, J.-J. Su, J.-Y. Huang, and I. A. Yu, "Pump-probe spectroscopy of cold ^{87}Rb atoms in various polarization configurations," *Phys. Rev. A* **63**, 043808 (2001).
42. J. Y. Courtois, "Spectroscopie Raman et Rayleigh stimulie d'atomes refroidis par laser: dynamique des mélasses optiques unidimensionnelles," Ph.D. dissertation (Ecole Polytechnique, 1993).